ON INTERPOLATION OF DIFFERENTIALLY STRUCTURED IMAGES

Hagai Kirshner and Moshe Porat

Department of Electrical Engineering, Technion–Israel Institute of Technology, Haifa 32000, Israel
phone: + (972) 4-8293283, fax: + (972) 4-8294709
email: kirshner@tx.technion.ac.il, web: http://visl.technion.ac.il/kirshner

Department of Electrical Engineering, Technion–Israel Institute of Technology, Haifa 32000, Israel
phone: + (972) 4-8294684, fax: + (972) 4-8295757
email: mp@ee.technion.ac.il, web: http://visl.technion.ac.il/mp

ABSTRACT

A vector space approach to image reconstruction is derived and introduced. The continuous-domain image is assumed to belong to a reproducing kernel Hilbert space and the sampling process is shown to correspond to an appropriate orthogonal projection. The values at the interpolating grid are shown to correspond to a set of inner product calculations, giving rise to a minimax solution for an ℓ_2 approximation problem. A tight upper bound on the ensued error is then derived and demonstrated. Examples of image resizing show that the proposed method yields better results than presently available methods, including the cubic B-spline method, in terms of SNR.

I. INTRODUCTION

Image interpolation is a fundamental task in image processing applications. Such applications include rotation, translation, resizing and derivative evaluation to name a few. The underlying idea in current interpolation methods corresponds to regularity properties that are assumed on the continuous-domain image. For example, a piecewise-polynomial model is often used, implying that the original continuous-domain image is smooth, up to a certain degree. Several interpolation methods such as nearest-neighbor, linear, Dodgson, Keys, Schaum, B-spline of higher orders, Meijering and o-MOMS assume such a model [1]–[5]. Furthermore, for a sufficiently smooth input signal, these very methods comply with the following upper bound on the approximation error

$$\left\|\mathbf{x}-\hat{\mathbf{x}}\right\|_{L_2} \leq C\cdot T^L \cdot \left\|\mathbf{x}^{(L)}\right\|_{L_2} \quad \text{as} \quad T\to 0. \tag{1}$$

Here, $\mathbf{x}$ is the original continuous-domain signal, $\hat{\mathbf{x}}$ is the interpolated signal and T is the sampling interval. In such a formulation, the parameters L and C are the approximation order and the proportional constant, respectively; they provide a means for comparing the various reconstruction (interpolation) methods. Recently, it was suggested to minimize the Sobolev norm of the reconstruction error instead of its L_2 norm; this approach was then applied to image reconstruction from singular points in a Gaussian scale space [6].

However, within the context of image processing applications, the interpolation stage yields a discrete-domain rather than a continuous-domain signal and no L_2 or Sobolev measures, but an l_2 measure, is to be considered instead.

In this work, an ℓ_2 interpolation method is derived and introduced for minimizing the maximum possible approximation error. Also, the piecewise-polynomial model is generalized by considering 2D Sobolev signals of finite support. Such an assumption on the continuous-domain image has been made in several image processing algorithms [7], [8] and it is adopted here as well. Within this setting, the ideal sampling process is shown to correspond to a set of inner product calculations; the same holds for the interpolated values. This signal representation interpretation to the sampling and to the interpolation processes gives rise to an alternative interpolation approach. A detailed analysis is given for the 1D case, followed by 2D scaling examples.

II. SAMPLING OF SMOOTH SIGNALS

We consider one-dimensional Sobolev spaces defined over a finite open support $\Omega=(-\pi,\pi)$. A Sobolev space of order p is denoted by $H_2^p(\Omega)$ and it consists of all finite energy functions for which their first p derivatives are of finite energy as well [9]. We adopt the following inner product

$$\left\langle \mathbf{x},\mathbf{y}\right\rangle_{H_2^p(\Omega)} = \sum_{n=0}^{p}\left\langle \mathbf{x}^{(n)},\mathbf{y}^{(n)}\right\rangle_{L_2(\Omega)}. \tag{2}$$

A Sobolev space is a reproducing kernel Hilbert space, suggesting an orthogonal projection interpretation for the ideal sampling process.

Lemma 1: The reproducing kernel of $H_2(\Omega)$ ($p=1$) is given by

$$K\left(s,t\right)=\frac{\cosh\left(\left|s-t\right|-\pi\right)}{2\sinh\left(\pi\right)}, \tag{3}$$

where $s,t\in\Omega$.

Proof: Let $\mathbf{x}\in H_2(\Omega)$ be an arbitrary function. Then, it can be expressed by

$$\mathbf{x}(s)=\sum_n a_n\cdot e^{jns}, \tag{4}$$

where equality holds point-wise. The sampled value $\mathbf{x}(t)$ is a linear bounded functional and by Riesz representation theorem can be expressed by means of an inner product calculation

$$\mathbf{x}(t)=\left\langle \mathbf{x}\left(s\right),K\left(s,t\right)\right\rangle_{H_2(\Omega)}. \tag{5}$$

Fixing the parameter t, one can express $K(s,t)$ by means of its Fourier coefficients b, yielding

$$\begin{aligned}\mathbf{x}(t) &= \sum_n a_n \cdot e^{jnt} \\ &= \int_\Omega x(s) \cdot \overline{K(s,t)}\, ds + \int_\Omega x'(s) \cdot \overline{K'(s,t)}\, ds \\ &= \sum_{n,m} a_n \overline{b}_m (1 + n \cdot m) \int_\Omega e^{j(n-m)s}\, ds \\ &= 2\pi \sum_n a_n \overline{b}_n (1+n^2). \end{aligned} \quad (6)$$

$\mathbf{x}$ is arbitrary yielding $b_n = (2\pi)^{-1} \cdot e^{-jnt}/(1+n^2)$. That is,

$$K(s,t) = \frac{1}{2\pi} \sum_n \frac{e^{jn(s-t)}}{1+n^2}. \quad (7)$$

Utilizing the Fourier transform relation $e^{-|t|} \xrightarrow{\mathcal{F}} 2/(1+\omega^2)$ and the aliasing effect occurring in the time domain, one can show the equivalence of this last expression with (3). □

Corollary 1: The reproducing kernel of $H_2^p(\Omega)$ is implicitly given by

$$K(s,t) = \frac{1}{2\pi} \sum_n \frac{e^{jn(s-t)}}{1+n^2+\ldots+n^{2p}}. \quad (8)$$

Let $\Lambda = \{t_n\}_{n=0,\ldots,N-1}$ be a finite set of sampling points. It then follows that the corresponding sampling kernels $\{K(s,t_n)\}_{n=0,\ldots,N-1}$ constitute a Riesz basis for their span (the values of a Sobolev function at distinct points are linearly independent)

$$\mathcal{S} = Span\left\{K(s,t_n)\right\}_{n=0}^{N-1}. \quad (9)$$

This sampling space is a subspace of $H_2^p(\Omega)$. The Gram matrix of these kernels can be shown to comply with

$$G(m,n) = K(t_m,t_n) \quad m,n = 0,\ldots,N-1. \quad (10)$$

The orthogonal projection of $\mathbf{x}$ onto the sampling space is given by

$$P_{\mathcal{S}}\mathbf{x} = \sum_{n=0}^{N-1} a_n \cdot K(\cdot,t_n), \quad (11)$$

where $a = G^{-1}c$ and c denotes the ideal samples of $\mathbf{x}$ according to Λ. The unknown portion of $\mathbf{x}$ that is not captured by the sampling process is $P_{\mathcal{S}^\perp}\mathbf{x} = \mathbf{x} - P_{\mathcal{S}}\mathbf{x}$.

III. INTERPOLATION

Interpolation is the task of evaluating a continuous-domain function at predefined points while having its sampled version at other points as the only available data. A common approach to this task relies on kernels that have attractive properties in terms of approximation order, of proportional constant and of minimal support (1). In this work, however, a different approach is taken in which an ℓ_2 rather than an L_2 measure is considered. Specifically, the interpolated values alone are compared with the true values while no continuous-domain approximation is considered. The motivation for such an approach stems from image processing applications for which the interpolation stage yields a discrete-domain rather than a continuous-domain signal.

Theorem 1: Let $\Lambda = \{t_n\}_{n=0\ldots N-1}$ be a sampling grid and let c be the ideal samples of $\mathbf{x} \in H_2^p(\Omega)$. Given $\tau \notin \Lambda$, the solution of

$$\arg\min_{\hat{\mathbf{x}}(\tau)\ c,\|\mathbf{x}\|_{H_2^p(\Omega)} \le L} \max \left|\mathbf{x}(\tau) - \hat{\mathbf{x}}(\tau)\right| \quad (12)$$

is given by

$$\hat{\mathbf{x}}(\tau) = c^T G^{-1} b, \quad (13)$$

where G is given by (10), $b_n = K(t_n,\tau)$ and K is given by (8). L is an arbitrary constant that complies with $L^2 \ge c^T G^{-1} c$.

Proof: Recalling Lemma 1, the value $\mathbf{x}(\tau)$ is given by

$$\mathbf{x}(\tau) = \left\langle \mathbf{x}(s),\, K(s,\tau) \right\rangle_{H_2^p(\Omega)}. \quad (14)$$

In addition, we recall that Λ defines a sampling space $\mathcal{S}$. Therefore, evaluating $\mathbf{x}(\tau)$ is equivalent to the approximation of (14) while having $P_{\mathcal{S}}\mathbf{x}$ as the only available data. This signal representation interpretation for the interpolation problem can be applied now to Theorem 1 of [10]. That is, the minimax solution of (12) is given by

$$\hat{\mathbf{x}}(\tau) = \left\langle P_{\mathcal{S}}\mathbf{x}(s),\, P_{\mathcal{S}}K(s,\tau) \right\rangle_{H_2^p(\Omega)}. \quad (15)$$

The sampling functions $\{K(s,t_n)\}$ constitute a Riesz basis for $\mathcal{S}$ and (13) follows accordingly. The constant L, upper-bounding the Sobolev norm of $\mathbf{x}$, is required for defining a robust minimax objective function [11]. □

Theorem 1 describes a minimax approach to interpolation. Given a point to be evaluated, it defines an interpolating kernel to be applied to the sampled data

$$k = G^{-1} b. \quad (16)$$

The support of this kernel may be as large as the size of the sampled data; that is, every sample value is significant to the interpolation task. Nevertheless, such kernels have in practice a relatively small support (Fig. 1); the reason for that resides in the structure of G^{-1} which has its significant values located near the main diagonal. As can be seen from Fig. 1, the support of k increases as the Sobolev order becomes larger. Also, the ensued minimax kernel for the case of $p = 1$ corresponds to the average of only the two adjacent samples (provided the interpolation point is located at the middle). The minimax solution of Theorem 1 is also element-wise optimal [11], implying that simultaneously designing several interpolation kernels can be performed separately, one kernel at a time. Theorem 1 also gives rise to an interpolating function. Let t_n be the n-th sampling point. Then,

$$\phi_n(t) = \sum_{m=0}^{N-1} G^{-1}_{n,m} \cdot K(t_m,t). \quad (17)$$

This interpolating function is applied to the sample value originating from t_n and it consists of a linear combination of the sampling kernels, i.e. $\phi \in \mathcal{S}$. Every sample point has its own interpolating function; if Λ is uniform, then the ensued interpolation functions resemble each other and posses a cyclic shift-invariant structure. Fig. 2 compares the proposed interpolating function with its B-spline counterpart for several Sobolev orders. Following Fig. 2(a), the minimax approach yields an interpolating function that is

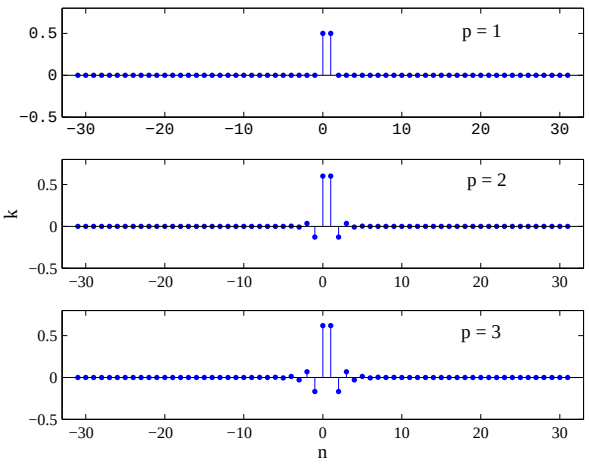

Fig. 1. Minimax interpolation kernels for Sobolev spaces. Here, the support of the functions is $\Omega = (-\pi, \pi)$, the sampling interval is $T = 0.1$ and the interpolating point is $\tau = 0.05$. The interpolation kernel k is given by (16) and it is depicted here for Sobolev orders of $p = 1, 2, 3$.

very similar to the hat B-spline function. However, these two functions are different as can be observed from the derivative of ϕ_n depicted therein as well. Furthermore, the minimax approach yields finite support functions regardless of the regularity constraint (i.e., Sobolev order) which is in contrast to B-spline interpolating functions. An upper bound on the approximation error is derived next.

Theorem 2: Let $\Lambda = \{t_n\}$ and $\Gamma = \{\tau_m\}$ be a sampling and an interpolation grid, respectively; and let $c \in \mathbb{R}^N$ and $d \in \mathbb{R}^M$ be the ideal samples of $\mathbf{x} \in H_2^p(\Omega)$ over Λ and Γ, respectively. Then,

$$\left\| d - \hat{d} \right\|_{\ell_2}^2 \leq B \cdot \left(\|\mathbf{x}\|_{H_2^p(\Omega)}^2 - c^T G^{-1} c \right), \qquad (18)$$

where $\hat{d}$ is the minimax approximation for d (Theorem 1), G is given by (10) and B is the largest eigenvalue of the matrix

$$H(k,l) = \\ = K(\tau_k, \tau_l) - \sum_{m,n=0}^{N-1} K(t_m, \tau_k) \cdot G^{-1}(m,n) \cdot K(t_n, \tau_l) \\ k, l = 0 \ldots M-1. \qquad (19)$$

Proof: We consider first a single interpolation point and identify the worst-case input signal possible. Clearly, this signal satisfies

$$\mathbf{x} = P_{\mathcal{S}}\mathbf{x} + P_{\mathcal{S}^\perp}\mathbf{x}, \qquad (20)$$

where $P_{\mathcal{S}}\mathbf{x}$ is a known continuous-domain signal and is given by (11). The approximation error is given by

$$\begin{aligned} \left| d - \hat{d} \right| &= \left| \langle P_{\mathcal{S}^\perp}\mathbf{x}, P_{\mathcal{S}^\perp} K(\cdot, \tau) \rangle_{H_2^p(\Omega)} \right| \\ &\leq \|P_{\mathcal{S}^\perp}\mathbf{x}\|_{H_2^p(\Omega)} \cdot \|P_{\mathcal{S}^\perp} K(\cdot, \tau)\|_{H_2^p(\Omega)} \end{aligned} \qquad (21)$$

where τ is the interpolating point. Now,

$$\begin{aligned} \|P_{\mathcal{S}^\perp}\mathbf{x}\|_{H_2^p(\Omega)}^2 &= \|\mathbf{x}\|_{H_2^p(\Omega)}^2 - c^T G^{-1} c \\ \|K(\cdot,\tau)\|_{H_2^p(\Omega)}^2 &= K(0,0) \\ \|P_{\mathcal{S}} K(\cdot,\tau)\|_{H_2^p(\Omega)}^2 &= \sum_{m,n} K(t_m, \tau) \cdot G^{-1}(m,n) \cdot K(t_n, \tau), \end{aligned}$$

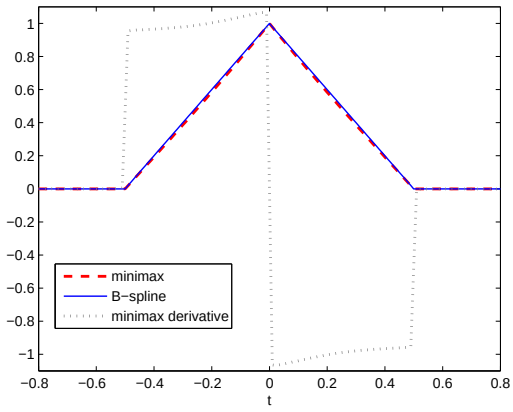

(a) Sobolev order $p = 1$.

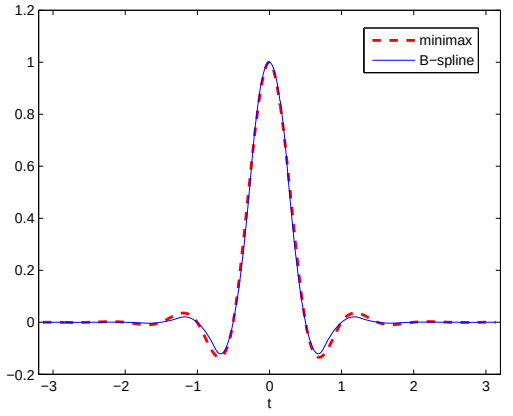

(b) Sobolev order $p = 2$.

Fig. 2. Minimax interpolating functions for Sobolev spaces. Here, the support of the functions is $\Omega = (-\pi, \pi)$ and the sampling interval is $T = 0.5$. The interpolating function is given by (17). Shown here is a comparison between the proposed interpolating function and the B-spline interpolating function. Here, p denotes the Sobolev order of the input signal.

and the upper bound for this single interpolation point follows immediately for the choice of

$$\begin{aligned} B &= \|P_{\mathcal{S}^\perp} K(\cdot,\tau)\|_{H_2^p(\Omega)}^2 \\ &= \|K(\cdot,\tau)\|_{H_2^p(\Omega)}^2 - \|P_{\mathcal{S}} K(\cdot,\tau)\|_{H_2^p(\Omega)}^2 \end{aligned} \qquad (22)$$

This upper bound is tight and is achieved by signals of the form

$$\mathbf{x} = P_{\mathcal{S}}\mathbf{x} + \alpha \cdot P_{\mathcal{S}^\perp} K(\cdot, \tau), \qquad (23)$$

where α is a scalar that determines the Sobolev norm of $\mathbf{x}$. When considering several interpolating points, the aproximation error is given by

$$\begin{aligned} \left\| d - \hat{d} \right\|_{\ell_2}^2 &= \sum_{m=0}^{M-1} |\langle P_{\mathcal{S}^\perp}\mathbf{x}, P_{\mathcal{S}^\perp} K(\cdot, \tau_m) \rangle|^2 \\ &\leq B \cdot \|P_{\mathcal{S}^\perp}\mathbf{x}\|_{H_2^p(\Omega)}^2, \end{aligned} \qquad (24)$$

where B is the upper frame bound of the functions $\{P_{\mathcal{S}^\perp} K(\cdot, \tau_m)\}_{m=0,\ldots,M-1}$ and is determined by the largest

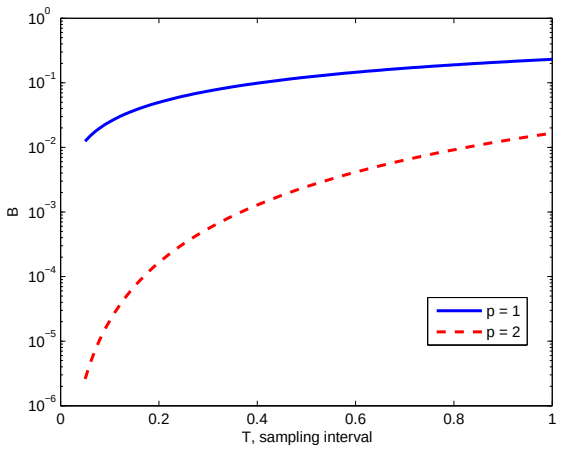

Fig. 3. An upper bound on the interpolation error, given by Theorem 2. Shown here is B for interpolating by a factor of two from a uniform sampling grid. As the sampling interval shortens, this portion of the upper bound tends to lower values. Here, p denotes the Sobolev order of the input signal.

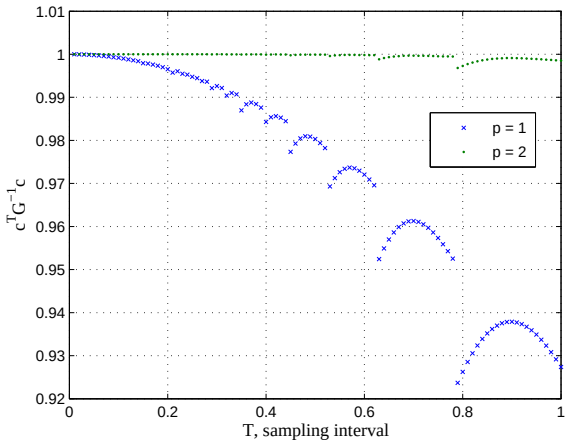

Fig. 4. An upper bound on the interpolation error, given by Theorem 2. Shown here is $\|P_{\mathcal{S}}\mathbf{x}\|^2 = c^T G^{-1} c$ for the case of $\mathbf{x} = (2\pi)^{-1/2}$ and for a uniform sampling grid. As the sampling interval shortens, this portion of the upper bound approaches the value of $\|x\|_{H_2^p(\Omega)} = 1$, where p denotes the Sobolev order of the input signal.

eigenvalue of their Gram matrix

$$\begin{aligned} H(k,l) &= \langle P_{\mathcal{S}^\perp} K(\cdot,\tau_k), P_{\mathcal{S}^\perp} K(\cdot,\tau_l)\rangle_{H_2^p(\Omega)} \\ &= \langle K(\cdot,\tau_k), P_{\mathcal{S}^\perp} K(\cdot,\tau_l)\rangle_{H_2^p(\Omega)} \\ &= \langle K(\cdot,\tau_k), K(\cdot,\tau_l) - P_{\mathcal{S}} K(\cdot,\tau_l)\rangle_{H_2^p(\Omega)} \end{aligned} \quad (25)$$

It then follows that the worst-case input signal achieving this upper bound is of the form

$$\mathbf{x} = P_{\mathcal{S}}\mathbf{x} + \sum_{m=0}^{M-1} \beta_m \cdot P_{\mathcal{S}^\perp} K(\cdot,\tau_m), \quad (26)$$

where β is the eigenvector corresponding to B that also guarantees the Sobolev norm of $\mathbf{x}$. □

As the sampling interval shortens, more information on $\mathbf{x}$ is available and one may expect the upper bound of Theorem 2 to become smaller. This characteristics is manifested in both B and $c^T G^{-1} c$. Fig. 3 depicts B as a function of the sampling interval for a uniform grid and for an interpolation by a factor of two. Fig. 4 depicts $\|P_{\mathcal{S}}\mathbf{x}\|^2 = c^T G^{-1} c$ in a similar manner for the case of $\mathbf{x} = (2\pi)^{-1/2}$; as the sampling interval shortens, this portion of the upper bound approaches the value of $\|x\|^2_{H_2^p(\Omega)} = 1$.

The generalization to images is carried out by considering 2D Sobolev functions. Let $\nu = (\nu_1, \nu_2)$ be a tuple of nonnegative integers where $|\nu| = \nu_1 + \nu_2$ and let

$$D^\nu = \frac{\partial^{\nu_1}}{\partial\alpha} \cdot \frac{\partial^{\nu_2}}{\partial\beta}. \quad (27)$$

We consider the two-dimensional Sobolev space of order $p \geq 2$ defined over a finite open support $\Omega = (-\pi,\pi) \times (-\pi,\pi)$ (unlike the 1D case, a 2D Sobolev space of order $p = 1$ is not a reproducing kernel Hilbert space). This space consists of functions $\mathbf{x}(\alpha,\beta)$ that satisfy $D^\nu \mathbf{x} \in L_2(\Omega)$ for all possible ν satisfying $|\nu| \leq p$. The corresponding inner product is given by [9]

$$\langle \mathbf{x}, \mathbf{y}\rangle_{H_2^p(\Omega)} = \sum_{\{\nu:\, 0 \leq |\nu| \leq p\}} \langle D^\nu \mathbf{x}, D^\nu \mathbf{y}\rangle_{L_2(\Omega)}. \quad (28)$$

This inner product gives rise to the following reproducing kernel

$$K(\alpha,\beta,x,y) = \frac{1}{4\pi^2} \sum_{n,m} \frac{e^{jn(\alpha-x)+jm(\beta-y)}}{\sum_{\{\nu:\, 0\leq|\nu|\leq p\}} n^{2\nu_1} m^{2\nu_2}}, \quad (29)$$

which is not separable in α and β. For example, a Sobolev order of $p = 2$ yields

$$K(\alpha,\beta,x,y) = \frac{1}{4\pi^2} \sum_{n,m} \frac{e^{jn(\alpha-x)+jm(\beta-y)}}{1 + n^2 + m^2 + n^2m^2 + n^4 + m^4}. \quad (30)$$

Next, the minimax approach is compared with the cubic B-spline approach. A uniform sampling grid is assumed and an interpolation by a factor of three is examined. Fig. 5 depicts a cervical Pap smear image. This image was downsampled by a factor of three and was then interpolated accordingly. The minimax interpolation approach, shown in Fig. 6, yields SNR=30[dB] while the well known cubic B-spline method yields only 29.7[dB]. Table I further compares the minimax and the cubic B-spline interpolation error for several additional images. The minimax method was designed for minimizing the ℓ_2 error and it is shown to yield better results in terms of SNR.

IV. CONCLUSIONS

An ℓ_2 approach to image reconstruction has been introduced. The continuous-domain images are assumed to belong to a reproducing kernel Hilbert space and the sampling process is shown to correspond to an appropriate orthogonal projection. It has been also shown that the values at the interpolating grid correspond to a set of inner product calculations, and that this signal representation interpretation can be utilized to derive a minimax solution for the corresponding ℓ_2 approximation problem. To provide a quantitative measure for the efficiency of the new method, a tight upper bound on the approximation error has been derived and demonstrated. Numerical examples show that the proposed interpolation method yields better results in

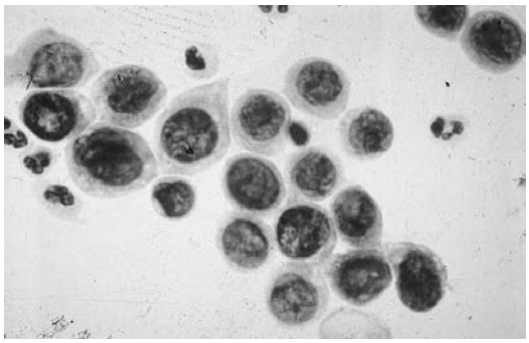

Fig. 5. A cervical Pap smear image.

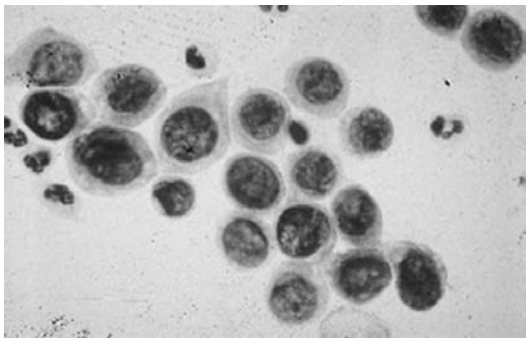

Fig. 6. Interpolation by a factor of three. The proposed approach, shown here for $p = 3$, yields SNR=30[dB] while the cubic B-spline interpolation method yields only 29.7[dB].

terms of SNR compared to presently available techniques, and could be useful in various practical applications.

ACKNOWLEDGEMENT

This work was supported in part by the HASSIP Research Program of the European Commission, by the H. & R. Sohnis Cardiology Research Fund, and by the Ollendorff Minerva Centre. Minerva is funded through the BMBF.

REFERENCES

[1] A. K. Jain, *Fundamentals of Digital Image Processing*. Englewood Cliffs, NJ: Prentice-Hall, 1989.

[2] T. M. Lehmann, C. Gönner, and K. Spitzer, "Survey: Interpolation methods in medical image processing," *IEEE Trans. Medical Imaging*, vol. 18, pp. 1049–1075, November 1999.

TABLE I

A COMPARISON OF INTERPOLATION METHODS BY A FACTOR OF THREE

Image		Cubic B-spline SNR (dB)	Minimax SNR (dB)
	Brain MRI	17.1	17.3
	Sailboat	21.5	21.7
	Man	20.4	20.6
	Fishing boat	20.3	20.4
	House	22.8	22.9
	Lena	24.4	24.5

[3] E. H. W. Meijering, K. J. Zuidervel, and M. A. Viergever, "Image reconstruction with symmetrical piecewise nth-order polynomial kernels," *IEEE Trans. Image Processing*, vol. 8, pp. 192–201, February 1999.

[4] P. Thévenaz, T. Blu, and M. Unser, "Interpolation revisited," *IEEE Trans. Medical Imaging*, vol. 19, pp. 739–758, July 2000.

[5] T. Blu, P. Thévenaz, and M. Unser, "Moms: Maximal-order interpolation of minimal support," *IEEE Trans. Image Processing*, vol. 10, pp. 1069–1080, July 2001.

[6] B. Janssen, F. Kanters, R. Duits, L. Florak, and B. ter Haar Romeny, "A linear image reconstruction framework based on Sobolev type inner products," *Int. J. Computer Vision*, vol. 70, no. 3, pp. 231–240, December 2006.

[7] D. Mumford and J. Shah, "Optimal approximations by piecewise smooth functions and associated variational problems," *Comm. Pure Applied. Math.*, vol. 42, pp. 577–685, 1989.

[8] L. Rudin, S. Osher, and E. Fatemi, "Nonlinear total variation based noise removal algorithms," *Physica D*, vol. 60, pp. 259–268, 1992.

[9] R. A. Adams, *Sobolev spaces*. New York, NY: Academic Press, 1975.

[10] H. Kirshner and M. Porat, "On the approximation of L_2 inner products from sampled data," *IEEE Trans. Signal Processing*, vol. 55, no. 5, pp. 2136–2144, May 2007.

[11] T. G. Dvorkind, H. Kirshner, Y. C. Eldar, and M. Porat, "Minimax approximation of representation coefficients from generalized samples," *accepted to IEEE Trans. Signal Processing*.